

# Charged Extracellular Residues, Conserved throughout a G-protein-coupled Receptor Family, Are Required for Ligand Binding, Receptor Activation, and Cell-surface Expression\*

Received for publication, August 10, 2006, and in revised form, September 8, 2006. Published, JBC Papers in Press, September 21, 2006, DOI 10.1074/jbc.M607639200

Stuart R. Hawtin<sup>†1,2</sup>, John Simms<sup>†1</sup>, Matthew Conner<sup>†</sup>, Zoe Lawson<sup>†</sup>, Rosemary A. Parslow<sup>†</sup>, Julie Trim<sup>§</sup>, Andrew Sheppard<sup>§</sup>, and Mark Wheatley<sup>†3</sup>

From the <sup>†</sup>School of Biosciences, University of Birmingham, Edgbaston, Birmingham B15 2TT, United Kingdom and <sup>§</sup>Ferring Research Ltd., Southampton Science Park, 1 Venture Road, Southampton SO16 7NP, United Kingdom

For G-protein-coupled receptors (GPCRs) in general, the roles of extracellular residues are not well defined compared with residues in transmembrane helices (TMs). Nevertheless, extracellular residues are important for various functions in both peptide-GPCRs and amine-GPCRs. In this study, the V<sub>1a</sub> vasopressin receptor was used to systematically investigate the role of extracellular charged residues that are highly conserved throughout a subfamily of peptide-GPCRs, using a combination of mutagenesis and molecular modeling. Of the 13 conserved charged residues identified in the extracellular loops (ECLs), Arg<sup>116</sup> (ECL1), Arg<sup>125</sup> (top of TMIII), and Asp<sup>204</sup> (ECL2) are important for agonist binding and/or receptor activation. Molecular modeling revealed that Arg<sup>125</sup> (and Lys<sup>125</sup>) stabilizes TMIII by interacting with lipid head groups. Charge reversal (Asp<sup>125</sup>) caused re-ordering of the lipids, altered helical packing, and increased solvent penetration of the TM bundle. Interestingly, a negative charge is excluded at this locus in peptide-GPCRs, whereas a positive charge is excluded in amine-GPCRs. This contrasting conserved charge may reflect differences in GPCR binding modes between peptides and amines, with amines needing to access a binding site crevice within the receptor TM bundle, whereas the binding site of peptide-GPCRs includes more extracellular domains. A conserved negative charge at residue 204 (ECL2), juxtaposed to the highly conserved disulfide bond, was essential for agonist binding and signaling. Asp<sup>204</sup> (and Glu<sup>204</sup>) establishes TMIII contacts required for maintaining the  $\beta$ -hairpin fold of ECL2, which if broken (Ala<sup>204</sup> or Arg<sup>204</sup>) resulted in ECL2 unfolding and receptor dysfunction. This study provides mechanistic insight into the roles of conserved extracellular residues.

G-protein-coupled receptors (GPCRs)<sup>4</sup> exhibit a common tertiary structure comprising seven transmembrane helices (TMs) linked by extracellular loops (ECLs) and intracellular loops. The atomic detail of this general GPCR fold has been elucidated for bovine rhodopsin (bRho) using x-ray crystallography (1). This confirmed that the chromophore 11-*cis*-retinal is covalently linked to Lys<sup>296(7.43)</sup> in transmembrane helix VII (TMVII) via a protonated Schiff-base and projects into a binding pocket formed within the TM bundle where it interacts with amino acid side chains and water molecules (1, 2).<sup>5</sup> Likewise, the binding pocket for small biogenic amine neurotransmitters such as acetylcholine and norepinephrine is buried deep within the TM bundle (3). Nevertheless, it is known from the bRho x-ray structure that the extracellular domains possess defined structure and are orientated to interact with each other and with the TM helices. Indeed ECL2 of bRho forms a  $\beta$ -hairpin that plunges down into the helical bundle to form a plug over the chromophore. Furthermore, the orientation of ECL2 in the majority of GPCRs is restrained by a conserved disulfide bond between ECL2 and the top of TMIII (1, 2).

The neurohypophysial peptide hormones vasopressin (AVP) and oxytocin (OT) generate a wide range of physiological effects, including vasopressor and antidiuretic and uterotonic actions (4, 5). The effects of AVP/OT are mediated by a family of receptors (V<sub>1a</sub>R, V<sub>1b</sub>R, V<sub>2</sub>R, and OTR), which together with the vasotocin receptor (VTR), mesotocin receptor, and isotocin receptor from lower vertebrates constitute a subfamily of the rhodopsin/ $\beta$ -adrenergic receptor class of GPCRs (family A). The V<sub>1a</sub>R, V<sub>1b</sub>R, and OTR couple to phospholipase C thereby generating inositol 1,4,5-trisphosphate and diacylglycerol as second messengers, whereas the V<sub>2</sub>R stimulates adenylyl cyclase. The V<sub>1a</sub>R is widely distributed and mediates nearly all of the actions of AVP with the exceptions of antidiuresis (V<sub>2</sub>R)

\* This work was supported by grants (to M. W.) from the Wellcome Trust, the Biotechnology and Biological Sciences Research Council, and Ferring Research. The costs of publication of this article were defrayed in part by the payment of page charges. This article must therefore be hereby marked "advertisement" in accordance with 18 U.S.C. Section 1734 solely to indicate this fact.

<sup>1</sup> Both authors should be considered as joint first authors.

<sup>2</sup> Present address: Novartis Pharma AG, WSJ-386.9.59, CH-4002 Basel, Switzerland.

<sup>3</sup> To whom correspondence should be addressed: School of Biosciences, University of Birmingham, Edgbaston, Birmingham, B15 2TT, UK. Tel.: 44-121-4143981; Fax: 44-121-414-5925; E-mail: m.wheatley@bham.ac.uk.

<sup>4</sup> The abbreviations used are: GPCR, G-protein-coupled receptor; AVP, [Arg<sup>8</sup>]vasopressin; bRho, bovine rhodopsin; CA, cyclic peptide antagonist; ECL, extracellular loop; HA, hemagglutinin; InsP, inositol phosphate; InsP<sub>3</sub>, inositol trisphosphate; LA, linear peptide antagonist; OT, oxytocin; OTR, oxytocin receptor; PhAc, phenylacetyl; TM, transmembrane helix; V<sub>1a</sub>R, V<sub>1a</sub> vasopressin receptor; V<sub>1b</sub>R, V<sub>1b</sub> vasopressin receptor; V<sub>2</sub>R, V<sub>2</sub> vasopressin receptor; VTR, vasotocin receptor; BSA, bovine serum albumin; PrBCM, propylbenzylcholine mustard.

<sup>5</sup> Residues in the TMs are referred to by residue number and the nomenclature of Ballosteros and Weinstein (53).

and ACTH secretion ( $V_{1a}R$ ). Activation of the OTR stimulates contraction of the uterine myometrium during labor and causes lactation. In addition to the characteristic architecture of GPCRs, members of the neurohypophysial peptide hormone receptor family share certain sequence motifs and exhibit related pharmacologies (5–7). The hormone-binding site of these receptors includes residues in the TM bundle (8) and ECL1 (9–11). It has also been reported that the N termini of the  $V_{1a}R$  and OTR are required for agonist binding (12, 13). In particular, two charged residues (Arg<sup>46</sup> and Glu<sup>54</sup>) in the  $V_{1a}R$  N terminus are required for high affinity agonist binding but not antagonist binding (14, 15). Likewise, Arg<sup>34</sup> in the N terminus of the OTR is required for agonist binding (16).

For GPCRs in general, the roles of extracellular residues are not well understood compared with residues in the TM domain. Nevertheless, extracellular residues are important for binding both amine (17) and peptide (18) ligands and have been implicated in ligand receptor-subtype specificity (19), binding allosteric modulators (20), switching ligand agonist/antagonist properties (21), and human immunodeficiency virus co-receptor activity (22). The aim of this study was to use the  $V_{1a}R$  to systematically investigate the function of extracellular charged residues that are highly conserved throughout a subfamily of peptide GPCRs. By using a combination of mutagenesis and molecular modeling, our results indicate that specific conserved charged residues in ECL1, ECL2, and ECL3 fulfill important roles in ligand binding, receptor activation, domain conformation, and cell-surface expression.

## EXPERIMENTAL PROCEDURES

**Materials**—AVP was purchased from Sigma. The cyclic peptide antagonist (CA) 1-( $\beta$ -mercapto- $\beta$ , $\beta$ -cyclopentamethylenepropionic acid), 2-(*O*-methyl)tyrosine AVP ( $d(CH_2)_5Tyr(Me)^2AVP$ ), and linear peptide antagonist (LA) phenylacetyl (PhAc)-D-Tyr(Me)<sup>2</sup>Arg<sup>6</sup>Tyr(NH<sub>2</sub>)<sup>9</sup>AVP were from Bachem (St. Helens, UK). SR 49059 was a gift from Sanofi Recherche (Toulouse, France). Cell culture media, buffers, and supplements were purchased from Invitrogen. Restriction enzymes were obtained from MBI Fermentas (Sunderland, UK).

**Mutant Receptor Constructs**—Mutation of the  $V_{1a}R$  was made using a PCR approach as described previously (15). The mutant receptor constructs [D112A] $V_{1a}R$ , [R116A] $V_{1a}R$ , [R118A] $V_{1a}R$ , [D121A] $V_{1a}R$ , and [R125A] $V_{1a}R$  were engineered using the antisense oligonucleotides as follows: 5'-GGC-AAA-C-**AC-CTG-CAG-GTG-CTT-CAC-CAC-GCG-GCA-CAG-CCA-GTC-GGG-CCC-GCG-GAA-GCG-GTA-GGT-GAT-GGC-C-CA-GC-3'**; 5'-GGC-AAA-C**AC-CTG-CAG-GTG-CTT-CAC-C-AC-GCG-GCA-CAG-CCA-GTC-GGG-CCC-GCG-GAA-GG-C-GTA-GG-3'**; 5'-GGC-AAA-C**AC-CTG-CAG-GTG-CTT-C-AC-CAC-GCG-GCA-CAG-CCA-GTC-GGG-CCC-GGC-GA-A-GCG-G-3'**; 5'-GGC-AAA-C**AC-CTG-CAG-GTG-CTT-CA-C-CAC-GCG-GCA-CAG-CCA-GGC-GGG-CCC-3'**; and 5'-G-GC-AAA-C**AC-CTG-CAG-GTG-CTT-CAC-CAC-GGC-G-CA-CAG-CCA-GTC-GGG-CCC-3'**, respectively. Each primer contained a unique SdaI restriction site (underlined) and base changes (shown in boldface) to generate each individual Ala substitution plus base changes to create a silent ApaI restriction site for diagnostic purposes (shown in italics). The same cloning

strategy was employed to generate the mutant constructs [D112E] $V_{1a}R$ , [D112K] $V_{1a}R$ , [D112R] $V_{1a}R$ , [R116D] $V_{1a}R$ , [R116E] $V_{1a}R$ , [R116K] $V_{1a}R$ , [R125D] $V_{1a}R$ , and [R125K] $V_{1a}R$  using the antisense oligonucleotides as follows: 5'-GGC-AAA-C**AC-CTG-CAG-GTG-CTT-CAC-CAC-GCG-GCA-CAG-C-CA-GTC-GGG-CCC-GCG-GAA-GCG-GTA-GGT-GAT-C-TC-CCA-GC-3'**; 5'-GGC-AAA-C**AC-CTG-CAG-GTG-CTT-CAC-CAC-GCG-GCA-CAG-CCA-GTC-GGG-CCC-GCG-GAA-GCG-GTA-GGT-GAT-TTT-CCA-GC-3'**; 5'-GGC-AAA-C**AC-CTG-CAG-GTG-CTT-CAC-CAC-GCG-GCA-C-AG-CCA-GTC-GGG-CCC-GCG-GAA-GCG-GTA-GGT-G-AT-GCG-CCA-GC-3'**; 5'-GGC-AAA-C**AC-CTG-CAG-GTG-CTT-CAC-CAC-GCG-GCA-CAG-CCA-GTC-GGG-C-CC-GCG-GAA-GTC-GTA-GGT-G-3'**; 5'-GGC-AAA-C**AC-CTG-CAG-GTG-CTT-CAC-CAC-GCG-GCA-CAG-CCA-GTC-GGG-CCC-GCG-GAA-CTC-GTA-GGT-G-3'**; 5'-GGC-AAA-C**AC-CTG-CAG-GTG-CTT-CAC-CAC-GCG-GCA-CAG-CCA-GTC-GGG-CCC-GCG-GAA-TTT-GTA-GGT-G-3'**; 5'-GGC-AAA-C**AC-CTG-CAG-GTG-CTT-CAC-CAC-GTC-GCA-CAG-CCA-GTC-GGG-CCC-3'**; and 5'-GGC-AA-A-C**AC-CTG-CAG-GTG-CTT-CAC-CAC-TTT-GCA-CA-G-CCA-GTC-GGG-CCC-3'**, respectively. PCR products were subcloned into the HA epitope-tagged rat  $V_{1a}R$  coding sequence in the mammalian expression vector pcDNA3.1 (Invitrogen) utilizing unique HindIII and SdaI restriction sites.

The mutations [E193A] $V_{1a}R$ , [E195A] $V_{1a}R$ , [K201A] $V_{1a}R$ , and [D204A] $V_{1a}R$  were made using antisense oligonucleotides as follows: 5'-GGC-GCG-**GGT-ACC-CCA-GGG-CTG-GAT-GAA-GGT-AGC-CCA-GCA-GTC-TTG-GGT-TTT-AGT-GCC-AT-T-GTT-CAC-CTC-GAT-TGC-GAT-CAC-AGA-G-3'**; 5'-GGC-GCG-**GGT-ACC-CCA-GGG-CTG-GAT-GAA-GGT-AGC-CCA-GCA-GTC-TTG-GGT-TTT-AGT-GCC-ATT-GTT-CA-C-CGC-GAT-TTC-G-3'**; 5'-GGC-GCG-**GGT-ACC-CCA-GGG-CTG-GAT-GAA-CGT-TGC-CCA-GCA-GTC-TTG-G-T-TGC-AGT-GCC-ATT-G-3'**; and 5'-GGC-GCG-**GGT-AC-C-CCA-GGG-CTG-GAT-GAA-GGT-AGC-CCA-GCA-GGC-TTG-GGT-TTT-AGT-GC-3'**, respectively. These primers contained the base changes (shown in boldface) to incorporate the Ala mutations and unique KpnI restriction site (underlined) used for subcloning. The [D204E] $V_{1a}R$  and [D204R] $V_{1a}R$  mutations were also engineered using this strategy using antisense oligonucleotides as follows: 5'-GGC-GCG-**GGT-ACC-CCA-GGG-CTG-G-AT-GAA-GGT-AGC-CCA-GCA-CTC-TTG-GGT-TTT-AGT-GC-3'** and 5'-GGC-GCG-**GGT-ACC-CCA-GGG-CTG-GAT-GAA-GGT-AGC-CCA-GCA-GCG-TTG-GGT-TTT-AGT-G-C-3'**. The construct [R216A] $V_{1a}R$  was made using sense oligonucleotide 5'-G-CCC-TGG-**GGT-ACC-GCC-GCG-TAC-GTG-ACC-TGG-ATG-ACC-TCA-GGT-GTC-TTC-GTG-G-3'**. This primer contained five base changes in the  $V_{1a}R$  sequence (shown in boldface) that created the Ala mutation (shown in italics) unique silent Pfl23II and Eco8II restriction sites (for diagnostic purposes) and a KpnI restriction site (underlined) for subcloning into the  $V_{1a}R$ .

The [E332A] $V_{1a}R$  mutation was made by PCR using both sense and antisense oligonucleotides. The sense primer was 5'-C-GAT-TCA-GCA-AAC-CCA-**TCGATA-ACA-ATC-ACG-GCG-3'**. This primer contained four base changes in the  $V_{1a}R$  sequence (indicated in boldface) that created a unique func-

## Conserved Exofacial Charged Residues

tional ClaI restriction site (underlined) without altering the amino acid sequence and incorporated the Glu<sup>332</sup> → Ala mutation (shown in italics). A KpnI/EcoRI digest of this PCR fragment was subcloned into the V<sub>1a</sub>R. The constructs [D323A]V<sub>1a</sub>R and [D330A]V<sub>1a</sub>R were made by PCR with pcDNA3-[E332A]V<sub>1a</sub>R as template. Mutant antisense oligonucleotides were 5'-CGT-GAT-TGT-TAT-CGA-TGG-GTT-TTC-TGA-ATC-GGT-CCA-GAT-GAA-ATT-CTC-AGC-CC-A-GAC-TGA-CC-3' and 5'-CGT-GAT-TGT-TAT-CGA-TGG-GTT-TTC-TGA-AGC-GGT-CCA-GAT-GAA-ATT-CTC-ATC-C-3' for [D323A]V<sub>1a</sub>R and [D330A]V<sub>1a</sub>R mutations, respectively. These primers contained base changes (shown in boldface) for the required Ala substitution and unique ClaI restriction site (underlined). The PCR products were subcloned into pcDNA3-[E332A]V<sub>1a</sub>R utilizing unique SdaI and ClaI restriction sites. All receptor constructs were confirmed by automated fluorescent sequencing (University of Birmingham, Birmingham, UK).

**Cell Culture and Transfection**—HEK 293T cells were routinely cultured in Dulbecco's modified Eagle's medium supplemented with 10% (v/v) fetal calf serum in humidified 5% (v/v) CO<sub>2</sub> in air at 37 °C. Cells were seeded at a density of ~5 × 10<sup>5</sup> cells/100-mm dish and transfected after 48 h using a calcium phosphate precipitation protocol with 10 μg of DNA/dish (16).

**Radioligand Binding Assays**—A washed cell membrane preparation of HEK 293T cells, transfected with the appropriate receptor construct, was prepared as described previously (23), and the protein concentration was determined using the BCA protein assay kit (Pierce) using bovine serum albumin as standard. Radioligand binding assays were performed as described previously (24) using either the natural agonist [Phe<sup>3</sup>-3,4,5-<sup>3</sup>H]AVP (0.5–1.5 nM), (64.2 Ci/mmol; PerkinElmer Life Sciences) or the V<sub>1a</sub>R-selective peptide antagonist [Phe<sup>3</sup>-3,4,5-<sup>3</sup>H]d(CH<sub>2</sub>)<sub>5</sub>Tyr(Me)<sup>2</sup>AVP (0.5–1.5 nM) (99 Ci/mmol; PerkinElmer Life Sciences) (25) as tracer ligand. Binding data were analyzed by nonlinear regression to fit theoretical Langmuir binding isotherms to the experimental data using PRISM Graphpad (Graphpad Software Inc., San Diego). Individual IC<sub>50</sub> values obtained for competing ligands were corrected for radioligand occupancy as described (26) using the radioligand affinity (K<sub>d</sub>) experimentally determined for each construct.

**Whole Cell Vasopressin V<sub>1a</sub> Receptor Binding**—HEK 293T cells were plated onto 12-well plates at a density of 2.5 × 10<sup>5</sup> cells/well in poly-D-lysine-coated 12-well plates and transfected after 24 h using Transfast<sup>TM</sup> (Promega Corp., Southampton, UK). After 36 h, each well received 0.5 ml of binding buffer (described above) containing 2% (w/v) BSA, 1–2 nM V<sub>1a</sub>R-selective peptide antagonist PhAc-D-Tyr(Me)<sup>2</sup>Arg<sup>6</sup>(3,4[<sup>3</sup>H]Pro)(3,5[<sup>3</sup>H]Tyr)<sup>9</sup>NH<sub>2</sub>-AVP (22 Ci/mmol; custom synthesis Phoenix Pharmaceuticals, INC. Belmont, CA) as tracer ligand in the presence (nonspecific) or absence (total) of 1 μM LA. Plates were incubated for 90 min at 37 °C, before removal of the medium by aspiration. After three rinses with ice-cold phosphate-buffered saline, 0.5 ml of 0.1 M NaOH was added to each well to extract radioactivity. After 15 min of incubation at 37 °C, the fluid from the plates was transferred to scintillation vials containing 10 ml of HiSafe3 scintillant mixture for counting. Cell-surface expression values were corrected for

radioligand occupancy as described (26) using the radioligand affinity (K<sub>d</sub>) experimentally determined for each construct.

**Determination of Cell-surface Expression Using Enzyme-linked Immunosorbent Assay**—All receptor constructs incorporated an HA epitope tag in the N terminus that enabled cell surface expression to be determined by enzyme-linked immunosorbent assay (27). Briefly, HEK 293T cells were seeded at a density of 1 × 10<sup>5</sup> cells/well in poly-D-lysine-coated 12-well plates and transfected after 24 h using Transfast<sup>TM</sup> (Promega Corp., Southampton, UK). After 36 h, cells were fixed with 3.7% (v/v) formaldehyde in TBS (20 mM Tris, pH 7.5, 150 mM NaCl) for 15 min at 37 °C and then washed three times with TBS. Nonspecific binding was blocked with 1% (w/v) BSA in TBS for 45 min. Anti-HA primary antibody (HA-7; Sigma) was diluted to 1:1000 in TBS containing 1% (w/v) BSA for 60 min at room temperature with occasional shaking, followed by three gentle washes with TBS. Cells were briefly re-blocked with 1% (w/v) BSA in TBS for 15 min, prior to incubation with secondary antibody (alkaline phosphatase-conjugated goat anti-mouse; Bio-Rad), and diluted to 1:3000 in 1% (w/v) BSA/TBS for 60 min with occasional shaking. Cells were washed three times with TBS before a colorimetric alkaline phosphate substrate (Bio-Rad) was added and incubated at 37 °C for 30 min. A 100-μl aliquot from each well was mixed with an equal volume of 0.4 M NaOH prior to measuring absorbance at 405 nm. Results were normalized against a wild-type control processed in parallel. Nontransfected cells were used to determine background. All experiments were performed in quadruplicate.

**AVP-induced Inositol Phosphates Production**—HEK 293T cells were seeded at a density of 2.5 × 10<sup>5</sup> cells/well in poly-D-lysine-coated 12-well plates and transfected after 24 h using Transfast<sup>TM</sup> (Promega). AVP-induced accumulation of inositol phosphates (InsPs) was assayed as described previously (12). Briefly, following pre-labeling of transfected cells with 2 μCi/ml *myo*-[2-<sup>3</sup>H]inositol (22.0 Ci/mmol; PerkinElmer Life Sciences) in inositol-free Dulbecco's modified Eagle's medium containing 1% (v/v) fetal calf serum, a mixed fraction containing mono-, bis-, and trisphosphates (InsP-InsP<sub>3</sub>) was collected following stimulation by AVP, at the concentrations indicated, in the presence of 10 mM LiCl.

**Molecular Modeling of the V<sub>1a</sub>R**—The V<sub>1a</sub>R sequence was aligned against the sequence corresponding to the crystal structure coordinates of bRho using ClustalW (28). The alignment was then used to generate homology models using MODELLER version 6.2 (29). A collection of 200 model structures was generated and ranked based on an objective function score provided by MODELLER version 6.2. From this ensemble, a single structure was selected for further analysis. Further refinement of the homology model was achieved through molecular dynamics (MD) simulations of the receptor embedded in a hydrated 1,2-dipalmitoyl-*sn*-glycero-3-phosphocholine bilayer. MD simulations were carried out using the GROMOS96 force-field parameters, with minor modifications, as implemented in GROMACS (30). Partial charges for the heavy atoms of Lys and Arg side chains were determined using the 6-31G basis set as implemented in GAMESS US.

A)	ECL1					ECL2			ECL3		
	112	116	118	121	125	195	204	216	323	330	332
rV <sub>1a</sub> R	W	D	I	T	R	E	I	E	D	E	D
mV <sub>1a</sub> R	W	D	I	T	R	E	I	E	D	E	D
vV <sub>1a</sub> R	W	D	I	T	R	E	I	E	D	E	D
sV <sub>1a</sub> R	W	D	I	T	R	E	I	E	D	E	D
huV <sub>1a</sub> R	W	D	I	T	R	E	I	E	D	E	D
rOTR	W	D	I	T	R	E	I	E	D	E	D
mOTR	W	D	I	T	R	E	I	E	D	E	D
vOTR	W	D	I	T	R	E	I	E	D	E	D
sOTR	W	D	I	T	R	E	I	E	D	E	D
huOTR	W	D	I	T	R	E	I	E	D	E	D
pOTR	W	D	I	T	R	E	I	E	D	E	D
bOTR	W	D	I	T	R	E	I	E	D	E	D
mkyOTR	W	D	I	T	R	E	I	E	D	E	D
rV <sub>2</sub> R	W	D	A	T	R	E	I	E	D	E	D
huV <sub>2</sub> R	W	K	A	T	R	E	I	E	D	E	D
bV <sub>2</sub> R	W	D	A	T	R	E	I	E	D	E	D
pV <sub>2</sub> R	W	D	A	T	R	E	I	E	D	E	D
dV <sub>2</sub> R	W	D	A	T	R	E	I	E	D	E	D
rV <sub>1b</sub> R	W	D	I	T	R	E	I	E	D	E	D
mV <sub>1b</sub> R	W	D	I	T	R	E	I	E	D	E	D
Mesotocin	W	D	I	T	R	E	I	E	D	E	D
Isotocin	W	D	I	T	R	E	I	E	D	E	D
Vasotocin	W	E	I	T	R	E	I	E	D	E	D

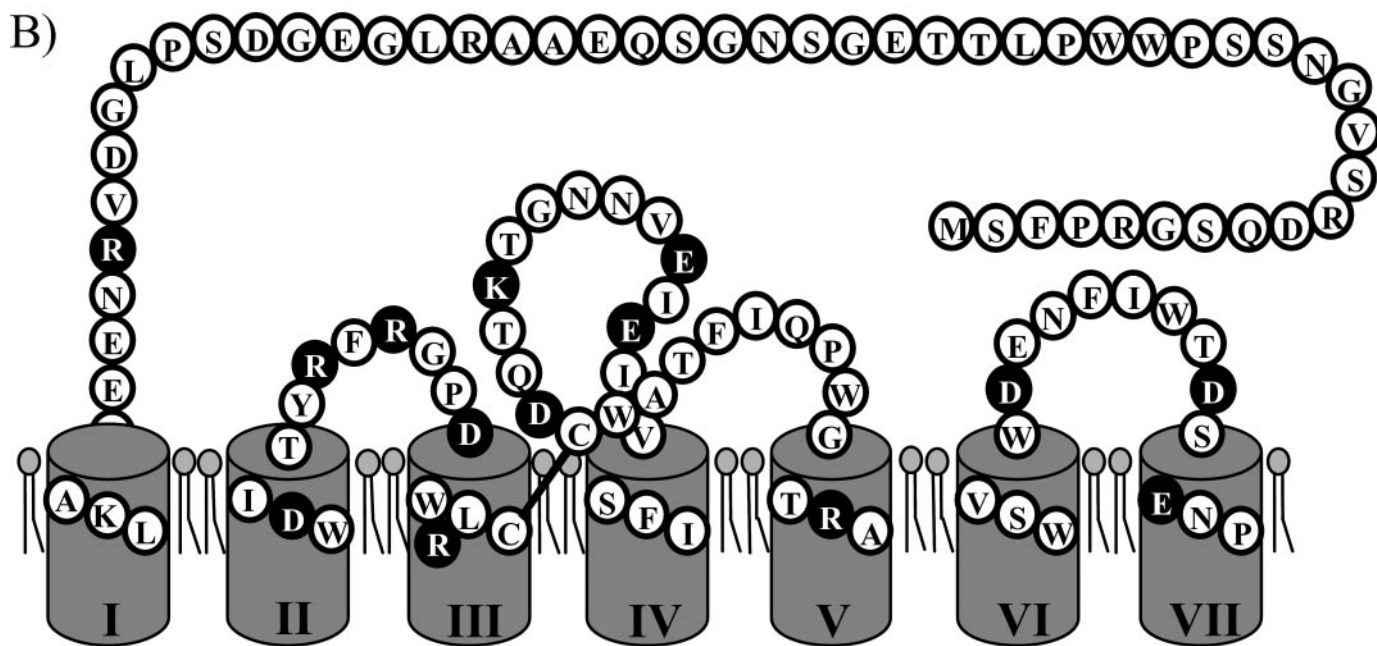


FIGURE 1. **The extracellular face of neurohypophysial hormone receptors.** A, sequence alignment of the extracellular loop regions of vasopressin and oxytocin receptors cloned from different species. The sequences of the extracellular loop regions (ECL1, ECL2, and ECL3) of the V<sub>1a</sub>R, OTR, V<sub>1b</sub>R, and V<sub>2</sub>R from different species have been aligned. The species of origin is indicated by a single letter code preceding the receptor subtype: r, rat; m, mouse; v, vole; s, sheep; h, human; p, pig; b, cow; mky, rhesus monkey; d, dog. Also shown is the sequence of the vasotocin and isotocin receptors from teleost fish and an amphibian mesotocin receptor. Conserved charged residues within these domains that were investigated in this study are boxed and numbered according to the rV<sub>1a</sub>R sequence. Sequences cited were obtained from Swiss Protein Database and GenEMBL. B, schematic diagram of the extracellular face of the rV<sub>1a</sub>R. Residues shown as white text on a black circle are the conserved charged residues investigated in this study.

## RESULTS

**Role of Charged Residues in the First Extracellular Loop (ECL1) of the V<sub>1a</sub>R**—The sequences of the extracellular loops, plus the extracellular boundaries, of the neurohypophysial peptide hormone subfamily of GPCRs are aligned in Fig. 1A. Within ECL1 (including the extracellular regions of TMII and

TMIII), there are five conserved charged residues as follows: Asp<sup>112</sup>, Arg<sup>116</sup>, Arg<sup>118</sup>, Asp<sup>121</sup>, and Arg<sup>125</sup> (Fig. 1B, residue number is based on rV<sub>1a</sub>R). Residues Arg<sup>116</sup>, Asp<sup>121</sup>, and Arg<sup>125</sup> are absolutely conserved across all VPR/OTRs cloned to date (Fig. 1A). Asp<sup>112</sup> is also conserved with the exception of the human V<sub>2</sub>R (Lys) and the VTR (Glu). Arg<sup>118</sup> is only conserved

## Conserved Exofacial Charged Residues

in  $V_{1a}R$ s, although positively charged residues are present at this locus in all  $V_2R$ s (Fig. 1A).

To assess the importance of these conserved residues in  $V_{1a}R$  function, each residue was substituted individually by Ala and then pharmacologically characterized using the natural agonist AVP and three different structural classes of antagonist as follows: (i) CA, [d(CH<sub>2</sub>)<sub>5</sub>Tyr(Me)<sup>2</sup>]AVP (25); (ii) LA ([PhAc-D-Tyr(Me)<sup>2</sup>Arg<sup>6</sup>Tyr(NH<sub>2</sub>)<sup>9</sup>]AVP (31)); and (iii) nonpeptide antagonist (SR 49059; (32)). The  $K_d$  values are presented in Table 1, corrected for radioligand occupancy. Mutating Arg<sup>116</sup>, Arg<sup>118</sup>, Asp<sup>121</sup>, or Arg<sup>125</sup> to Ala had only a slight effect on the binding of the agonist AVP or the three different classes of antagonist (Table 1 and Fig. 2). [D112A] $V_{1a}R$  was also essentially wild type, although the  $K_d$  value for LA was slightly (5-fold) increased. Furthermore, the mutations [D112A] $V_{1a}R$ , [R118A] $V_{1a}R$ , and [D121A] $V_{1a}R$  had little effect on signaling, with EC<sub>50</sub> values for AVP-stimulated inositol phosphate (InsP-InsP<sub>3</sub>) accumulations comparable with wild-type  $V_{1a}R$  (Table 1). In contrast, [R116A] $V_{1a}R$  and [R125A] $V_{1a}R$  had a marked effect on signaling, increasing the EC<sub>50</sub> value 70- and 16-fold, respectively, compared with the wild type (Fig. 3, A and B).

**A Positive Charge Is Required at Residue 116 in ECL1**—The charge requirements of residue 116 were investigated further by engineering [R116D] $V_{1a}R$ , [R116E] $V_{1a}R$  (incorporating a negative charge), and [R116K] $V_{1a}R$  (maintaining a positive charge). A negative charge was not tolerated at this position, as the affinity of AVP decreased 1600- and 730-fold for [R116D] $V_{1a}R$  and [R116E] $V_{1a}R$ , respectively, compared with wild-type  $V_{1a}R$  (Fig. 2A). In contrast, the binding affinities of the three different antagonists to [R116D] $V_{1a}R$  and [R116E] $V_{1a}R$  were relatively unchanged, although a small decrease (~6-fold) was observed for CA (Table 1). Incorporating a negative charge at this locus also perturbed receptor activation, increasing the EC<sub>50</sub> value for [R116D] $V_{1a}R$  and [R116E] $V_{1a}R$  by 53- and 23-fold, respectively (Fig. 3A). In contrast, maintaining a positive charge at this position ([R116K] $V_{1a}R$ ) resulted in a receptor that exhibited essentially wild-type binding (Fig. 2A and Table 1) and signaling (Fig. 3A).

**A Positive Charge Is Required at Residue 125 in ECL1**—The charge requirements of residue 125 were investigated further. Retaining a positive charge ([R125K] $V_{1a}R$ ) resulted in a wild-type receptor profile (Table 1). In contrast, introduction of a negative charge at this locus ([R125D] $V_{1a}R$ ) ablated specific binding of the radio-tracers (agonist and antagonist) and impaired signaling, with a marked decrease in AVP potency compared with wild-type  $V_{1a}R$  (Fig. 3B). Molecular modeling of the  $V_{1a}R$  indicated that Arg<sup>125</sup> orientates into the lipid bilayer (Fig. 4A), with the side-chain methylene groups interacting with the lipid hydrocarbon tails and the guanidinium group interacting with the lipid phosphate head groups and solvent. These contacts are preserved in [R125K] $V_{1a}R$ , consistent with the wild-type characteristics of this mutant receptor. In contrast, molecular dynamics of [R125D] $V_{1a}R$  revealed a re-ordering of the phospholipids in this region resulting from mutual repulsion between the negatively charged lipid phosphate head group and the carboxyl of the Asp side chain. This re-ordering of the lipids increased solvent accessibility at the extracellular end of TMIII and TMIV (Fig. 4A).

**Species-specific and Receptor Subtype-specific Differences at Position 112 in ECL1**—An Asp is highly conserved at residue 112 throughout this family of GPCRs, with the exception of the VTR and the human  $V_2R$  that possess Glu and Lys, respectively (Fig. 1). Pharmacological differences arising from this sequence variation were assessed. Conservative substitution ([D112E] $V_{1a}R$ ) resulted in wild-type binding and intracellular signaling, with only a small change in affinity for the CA antagonist (3-fold). Reversing the charge in [D112K] $V_{1a}R$  also slightly decreased the affinity of CA (5-fold) and reduced the affinity of the linear antagonist LA 8-fold (Table 1) but was otherwise wild type (Fig. 3C). However, in marked contrast to [D112K] $V_{1a}R$ , the construct [D112R] $V_{1a}R$  exhibited low affinity for AVP (Fig. 2B) and perturbed signaling (Fig. 3C). These effects were not because of a nonspecific disruption of the receptor tertiary fold as the affinity of the three classes of antagonist was unchanged (Table 1).

Asp<sup>112</sup> is located at the membrane/solvent interface at the extracellular end of TMII. Molecular modeling shows that when residue 112 is Glu or Lys, they occupy a similar position to Asp<sup>112</sup>, consistent with the near wild-type profile observed with these constructs. However, the increased side-chain length of Arg<sup>112</sup> compared with Lys<sup>112</sup> positions the positively charged guanidinium moiety of Arg<sup>112</sup> 3.0 Å from the carboxyl group of Glu<sup>54(1.35)</sup> (top of TMI), resulting in a charge-charge interaction between these two residues (Fig. 4B). A comparable interaction between the amine of Lys<sup>112</sup> and Glu<sup>54</sup> is far less likely as the functional groups are further apart (4.8 Å). Furthermore, the guanidinium of Arg has higher partial charges on its heavy atoms compared with the amine of Lys, which increases the potential of the Arg guanidinium to establish ionic interactions compared with the amine of Lys. In addition, the planar nature of the guanidinium group may aid directive interactions.

**Role of Charged Residues in the 2nd Extracellular Loop (ECL2) of the  $V_{1a}R$** —The ECL2 domain (including the extracellular borders of TMIV and TMV) of the  $V_{1a}R$  contains five charged residues Glu<sup>193</sup>, Glu<sup>195</sup>, Lys<sup>201</sup>, Asp<sup>204</sup>, and Arg<sup>216</sup> (Fig. 1B). Sequence analysis of ECL2 revealed the following: (i) charged residues are well conserved at loci corresponding to Glu<sup>195</sup>, Asp<sup>204</sup>, and Arg<sup>216</sup> throughout the vertebrate VPR/OTR family, whereas Glu<sup>193</sup> and Lys<sup>201</sup> are found only in the  $V_{1a}R$  subtype; (ii) Asp<sup>204</sup> is absolutely conserved with the single exception of the chick VTR, which has a Glu (33); (iii) a negative charge (usually a Glu but an Asp in  $V_2R$ s) is conserved at residue 195 with the exception of the human  $V_2R$ , which has Asn; and (iv) a positive charge (Arg/Lys) is conserved at position 216 but is replaced by a Pro in the sheep  $V_{1a}R$  (Fig. 1A).

To assess the functional importance of these conserved charged residues, each residue was mutated individually to Ala, and the pharmacological characteristics were compared with wild-type  $V_{1a}R$  (Table 1). With the exception of [D204A] $V_{1a}R$ , all the mutant constructs exhibited binding and signaling characteristics similar to wild type (Table 1). In marked contrast, [D204A] $V_{1a}R$  possessed a marked decrease in AVP affinity (2300-fold; Fig. 2C and Table 1) and impaired signaling (Fig. 3D). The affinity of [D204A] $V_{1a}R$  for the cyclic and nonpeptide antagonists remained unchanged (Table 1), indicating that the receptor protein was folded appropriately; nevertheless, the  $K_d$

TABLE 1

Pharmacological profile of mutant V<sub>1a</sub>R<sub>s</sub>

Mutant V<sub>1a</sub>R<sub>s</sub> were expressed in HEK 293T cells and characterized pharmacologically. Dissociation constants ( $K_d$ ) were calculated from IC<sub>50</sub> values and corrected for radioligand occupancy as described under "Experimental Procedures." Data shown are the mean  $\pm$  S.E. ( $n = 3$ ) of three replicates. SR 49059 indicates nonpeptide antagonist. EC<sub>50</sub> and E<sub>max</sub> values of AVP-induced accumulation of InsP-InsP<sub>3</sub> in cells expressing wild-type (WT) and mutant receptors are shown. Values shown are the mean  $\pm$  S.E. of three separate experiments performed in triplicate. NS indicates no stimulation. \*, data were taken from Ref. 34. Basal values (mean  $\pm$  S.E.) were 1217  $\pm$  252, 1263  $\pm$  224, 1135  $\pm$  201, 1080  $\pm$  158, 1214  $\pm$  207, 1073  $\pm$  223, 984  $\pm$  198, 956  $\pm$  214, 1075  $\pm$  248, 1256  $\pm$  258, 1208  $\pm$  174, 1007  $\pm$  125, 1283  $\pm$  202, 1321  $\pm$  230, 1299  $\pm$  188, 1116  $\pm$  207, 1302  $\pm$  191, 1350  $\pm$  260, 956  $\pm$  239, 1150  $\pm$  176, 1045  $\pm$  115, 1263  $\pm$  239, 1371  $\pm$  206, 1298  $\pm$  117, 1228  $\pm$  223, 1008  $\pm$  182, and 1251  $\pm$  248 dpm for wild type, [D112A]V<sub>1a</sub>R, [D112E]V<sub>1a</sub>R, [D112K]V<sub>1a</sub>R, [D112R]V<sub>1a</sub>R, [D116A]V<sub>1a</sub>R, [D116D]V<sub>1a</sub>R, [D116E]V<sub>1a</sub>R, [D116K]V<sub>1a</sub>R, [R118A]V<sub>1a</sub>R, [D121A]V<sub>1a</sub>R, [R125A]V<sub>1a</sub>R, [R125D]V<sub>1a</sub>R, [R125K]V<sub>1a</sub>R, [E193A]V<sub>1a</sub>R, [E195A]V<sub>1a</sub>R, [D204A]V<sub>1a</sub>R, [D204E]V<sub>1a</sub>R, [D204R]V<sub>1a</sub>R, [K201A]V<sub>1a</sub>R, [R216A]V<sub>1a</sub>R, [R46D]V<sub>1a</sub>R, [R46D/D204R]V<sub>1a</sub>R, [R125D/D204R]V<sub>1a</sub>R, [D323A]V<sub>1a</sub>R, [D330A]V<sub>1a</sub>R, and [E332A]V<sub>1a</sub>R respectively. None of the mutant receptors displayed constitutive activity. Cell-surface expression was determined, mean  $\pm$  S.E. ( $n = 3$ ), in parallel experiments as a percentage relative to wild-type V<sub>1a</sub>R using an ELISA-based assay, or as pmol/mg protein ( $B_{max}$ ) using whole cell <sup>3</sup>H-labeled LA binding where possible, as described under "Experimental Procedures."

Receptor Constructs	Binding affinities $K_d$ (nM)				Stimulation of InsP – InsP <sub>3</sub>		Cell-surface expression (%WT) (pmol/mg)
	AVP	CA	LA	SR 49059	EC <sub>50</sub> values (nM)	E <sub>max</sub> values (fold)	
WT	1.0 $\pm$ 0.1	0.7 $\pm$ 0.3	0.5 $\pm$ 0.1	1.9 $\pm$ 0.3	0.4 $\pm$ 0.2	8 $\pm$ 1.9	100 (1.7 $\pm$ 0.5)

## ECL1

Asp <sup>112</sup>	A	2.2 $\pm$ 0.9	2.1 $\pm$ 0.7	2.6 $\pm$ 0.7	2.0 $\pm$ 1.4	1.3 $\pm$ 0.4	4.1 $\pm$ 1.0	102 $\pm$ 6 (1.9 $\pm$ 0.6)
	E	2.3 $\pm$ 0.5	2.3 $\pm$ 0.5	0.6 $\pm$ 0.7	2.5 $\pm$ 1.2	1.1 $\pm$ 0.4	6.4 $\pm$ 0.5	87 $\pm$ 9 (1.3 $\pm$ 0.5)
	K	2.0 $\pm$ 0.7	3.9 $\pm$ 0.4	3.8 $\pm$ 0.5	3.4 $\pm$ 0.4	1.2 $\pm$ 0.1	4.2 $\pm$ 0.3	109 $\pm$ 1 (1.7 $\pm$ 0.6)
	R	390 $\pm$ 58	1.4 $\pm$ 0.1	2.3 $\pm$ 0.3	2.0 $\pm$ 0.2	4.6 $\pm$ 1.6	7.8 $\pm$ 1.6	98 $\pm$ 4 (1.6 $\pm$ 0.5)
Arg <sup>116</sup>	A	3.4 $\pm$ 0.7	1.8 $\pm$ 0.3	0.6 $\pm$ 0.3	4.8 $\pm$ 0.3	28 $\pm$ 1.2	5.4 $\pm$ 1.8	89 $\pm$ 3 (1.3 $\pm$ 0.3)
	D	1600 $\pm$ 250	4.6 $\pm$ 1.8	1.5 $\pm$ 0.2	5.6 $\pm$ 0.1	21 $\pm$ 1.6	4.2 $\pm$ 0.6	92 $\pm$ 4 (1.4 $\pm$ 0.6)
	E	730 $\pm$ 90	4.7 $\pm$ 1.1	0.5 $\pm$ 0.1	4.8 $\pm$ 0.6	9 $\pm$ 1.8	6.8 $\pm$ 1.3	95 $\pm$ 2 (1.8 $\pm$ 0.7)
	K	3.8 $\pm$ 0.7	1.6 $\pm$ 0.4	0.4 $\pm$ 0.3	3.2 $\pm$ 1.0	0.7 $\pm$ 0.5	5.2 $\pm$ 1.2	99 $\pm$ 2 (1.6 $\pm$ 0.5)
R118A		2.6 $\pm$ 0.5	0.7 $\pm$ 0.3	0.6 $\pm$ 0.1	4.4 $\pm$ 0.8	1.3 $\pm$ 0.5	6.9 $\pm$ 1.4	110 $\pm$ 3 (2.0 $\pm$ 0.7)
D121A		0.8 $\pm$ 0.4	0.7 $\pm$ 0.1	0.1 $\pm$ 0.1	3.7 $\pm$ 0.1	1.2 $\pm$ 0.3	7.0 $\pm$ 1.2	100 $\pm$ 3 (1.7 $\pm$ 0.6)
Arg <sup>125</sup>	A	3.4 $\pm$ 0.1	1.7 $\pm$ 0.5	0.5 $\pm$ 0.1	4.4 $\pm$ 0.7	6.5 $\pm$ 0.9	5.8 $\pm$ 0.3	56 $\pm$ 2 (0.7 $\pm$ 0.3)
	D	No [ <sup>3</sup> H]AVP, [ <sup>3</sup> H]CA, [ <sup>3</sup> H]LA binding detected				41 $\pm$ 1.1	2.4 $\pm$ 0.1	47 $\pm$ 2
	K	1.1 $\pm$ 0.2	0.7 $\pm$ 0.1	0.5 $\pm$ 0.2	2.3 $\pm$ 0.7	1.1 $\pm$ 0.1	5.2 $\pm$ 0.7	104 $\pm$ 2 (1.7 $\pm$ 0.5)

## ECL2

E193A	1.9 $\pm$ 0.3	0.9 $\pm$ 0.3	1.2 $\pm$ 0.1	0.3 $\pm$ 0.1	0.3 $\pm$ 0.1	5.1 $\pm$ 0.1	110 $\pm$ 5 (2.1 $\pm$ 0.5)
E195A	1.3 $\pm$ 0.1	0.9 $\pm$ 0.1	0.2 $\pm$ 0.1	4.0 $\pm$ 0.5	1.0 $\pm$ 0.1	7.9 $\pm$ 0.7	100 $\pm$ 1 (1.8 $\pm$ 0.4)
Asp <sup>204</sup>	A	2300 $\pm$ 240	2.0 $\pm$ 0.4	10 $\pm$ 3.4	1.3 $\pm$ 1.2	7.0 $\pm$ 1.3	56 $\pm$ 1
	E	1.6 $\pm$ 0.4	0.6 $\pm$ 0.2	0.4 $\pm$ 0.2	1.6 $\pm$ 0.6	0.8 $\pm$ 0.2	74 $\pm$ 3 (1.0 $\pm$ 0.4)
	R	2600 $\pm$ 680	4.4 $\pm$ 0.8	12 $\pm$ 1.2	1.6 $\pm$ 0.1	39 $\pm$ 1.0	4.2 $\pm$ 0.8
K201A	1.4 $\pm$ 0.3	0.4 $\pm$ 0.4	0.7 $\pm$ 0.3	1.4 $\pm$ 0.3	0.3 $\pm$ 0.1	8.7 $\pm$ 1.5	66 $\pm$ 3 (1.3 $\pm$ 0.3)
R216A	1.3 $\pm$ 0.1	1.2 $\pm$ 0.1	0.5 $\pm$ 0.1	1.3 $\pm$ 0.2	0.3 $\pm$ 0.1	6.1 $\pm$ 0.3	101 $\pm$ 4 (1.4 $\pm$ 0.4)
R46D*	1800 $\pm$ 380	0.5 $\pm$ 0.1	0.2 $\pm$ 0.1	2.1 $\pm$ 0.8	164 $\pm$ 49	2.4 $\pm$ 0.5	106 $\pm$ 6 (1.9 $\pm$ 0.5)
R46D/D204R	2500 $\pm$ 880	5.7 $\pm$ 2.6	15 $\pm$ 2.5	2.9 $\pm$ 0.8	>10 $\mu$ M	NS	20 $\pm$ 3
R125D/D204R	No [ <sup>3</sup> H]AVP, [ <sup>3</sup> H]CA or [ <sup>3</sup> H]LA binding detected				>10 $\mu$ M	NS	13 $\pm$ 7

## ECL3

D323A	1.2 $\pm$ 0.1	0.6 $\pm$ 0.1	0.4 $\pm$ 0.1	1.6 $\pm$ 0.2	1.2 $\pm$ 0.1	4.8 $\pm$ 0.5	52 $\pm$ 3 (0.6 $\pm$ 0.2)
D330A	1.8 $\pm$ 0.1	1.5 $\pm$ 0.3	0.6 $\pm$ 0.1	2.6 $\pm$ 0.2	1.8 $\pm$ 0.1	6.4 $\pm$ 0.4	91 $\pm$ 4 (1.9 $\pm$ 0.5)
E332A	2.3 $\pm$ 0.4	0.7 $\pm$ 0.1	0.4 $\pm$ 0.1	1.3 $\pm$ 0.1	1.6 $\pm$ 0.2	7.6 $\pm$ 0.1	102 $\pm$ 5 (1.7 $\pm$ 0.3)

## Conserved Exofacial Charged Residues

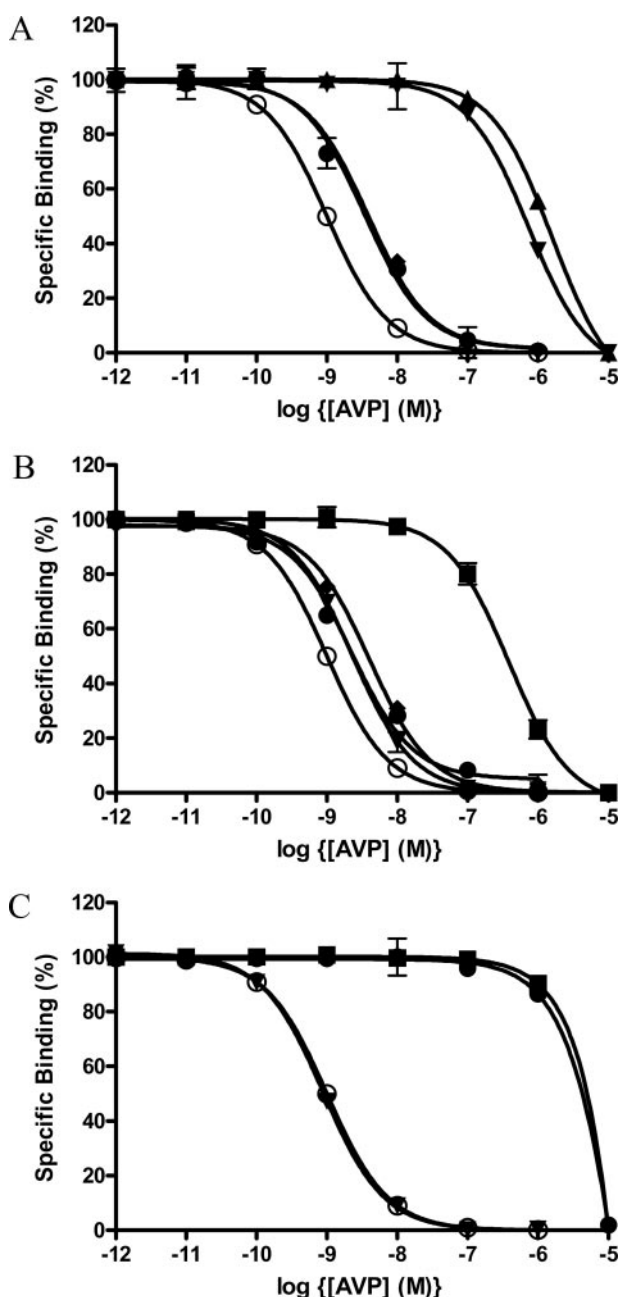


**FIGURE 2. Pharmacological characterization of ECL mutant receptors.** Radioligand binding studies with AVP as competing ligand were performed using a membrane preparation of HEK 293T cells transiently transfected as follows. *A*, wild-type (Arg<sup>116</sup>) V<sub>1a</sub>R (○); [R116A]V<sub>1a</sub>R (●); [R116E]V<sub>1a</sub>R (▼); [R116D]V<sub>1a</sub>R (▲); and [R116K]V<sub>1a</sub>R (◆). *B*, wild-type (Asp<sup>112</sup>) V<sub>1a</sub>R (○); [D112A]V<sub>1a</sub>R (●); [D112E]V<sub>1a</sub>R (▼); [D112K]V<sub>1a</sub>R (◆); and [D112R]V<sub>1a</sub>R (■). *C*, wild-type (Asp<sup>204</sup>) V<sub>1a</sub>R (○); [D204A]V<sub>1a</sub>R (●); [D204E]V<sub>1a</sub>R (▼); and [D204R]V<sub>1a</sub>R (■). Data are the mean ± S.E. of three separate experiments each performed in triplicate using [<sup>3</sup>H]AVP (0.5–1.5 nM) or <sup>3</sup>H-labeled CA (0.5–1.5 nM) as tracer. Values are expressed as percent specific binding, where non-specific binding was defined by d(CH<sub>2</sub>)<sub>5</sub>Tyr(Me)<sup>2</sup>AVP (1 μM). A theoretical Langmuir binding isotherm has been fitted to the experimental data as described under “Experimental Procedures.”

value for LA was increased 20-fold relative to wild type (Table 1). The charge requirements at position 204 were investigated. Retaining a negative charge ([D204E]V<sub>1a</sub>R) resulted in wild-type ligand binding and signaling (Figs. 2C and 3D and Table 1), whereas reversing the charge ([D204R]V<sub>1a</sub>R) markedly decreased both AVP affinity (Fig. 2C) and signaling (Fig. 3D)

and to a lesser extent LA and CA affinity (24- and 6-fold, respectively; Table 1). The binding of the nonpeptide antagonist to [D204R]V<sub>1a</sub>R was wild type.

*Investigating a Possible Interaction between Asp<sup>204</sup> and Arg<sup>125</sup> or Arg<sup>46</sup>*—Mutagenesis of Asp<sup>204</sup> or Arg<sup>125</sup> generated similar effects. Consequently, substitution by Ala ([D204A]V<sub>1a</sub>R and [R125A]V<sub>1a</sub>R) decreased the potency of AVP signaling by ~20-fold compared with wild-type V<sub>1a</sub>R (Fig. 3, D and B, respectively), and reversing the charge ([D204R]V<sub>1a</sub>R and [R125D]V<sub>1a</sub>R) increased the EC<sub>50</sub> 100-fold compared with wild-type V<sub>1a</sub>R. Although Arg<sup>125</sup> (top of TMIII) and Asp<sup>204</sup> (ECL2) are in different domains, they are located at opposite ends of the highly conserved disulfide bond and therefore in close proximity and spatially constrained. It was possible that a mutual charge interaction existed between these two residues, which was required for receptor activation. However, the double-reciprocal mutant [R125D/D204R]V<sub>1a</sub>R did not bind <sup>3</sup>H-labeled tracer ligands, did not signal when challenged with AVP (>10 μM), and was poorly expressed (Table 1). Consequently, these data do not support a mutual interaction between Arg<sup>125</sup> and Asp<sup>204</sup>.

We have established previously that a single residue (Arg<sup>46</sup>) located within the distal N terminus of the V<sub>1a</sub>R is critical for binding AVP but not peptide or nonpeptide antagonists (14) and that reversing the charge at this locus ([R46D]V<sub>1a</sub>R or [R46E]V<sub>1a</sub>R) impaired receptor function (34) in a similar manner to that observed for [D204R]V<sub>1a</sub>R in this study. Given that high affinity agonist binding required both Arg<sup>46</sup> and Asp<sup>204</sup>, it was feasible that a direct intra-molecular ionic interaction between Arg<sup>46</sup> and Asp<sup>204</sup> may contribute to high affinity agonist binding and receptor activation. However, the double-reciprocal mutant [R46D/D204R]V<sub>1a</sub>R bound AVP with very low affinity ( $K_d = 2500$  nM), a similar affinity to [R46D]V<sub>1a</sub>R or [D204R]V<sub>1a</sub>R (Table 1), and the signaling capability of [R46D/D204R]V<sub>1a</sub>R was also severely compromised. The overall tertiary fold of the receptor was nevertheless good as the nonpeptide antagonist bound with wild-type affinity, and the peptide antagonists CA and LA also bound with high affinity, albeit less than wild type (Table 1). Cell-surface expression of [R46D/D204R]V<sub>1a</sub>R was only ~20% of wild type. These data do not provide evidence for a direct interaction between Arg<sup>46</sup> and Asp<sup>204</sup>.

Molecular modeling indicated that Asp<sup>204</sup> lies at the center of a pocket defined by residues Lys<sup>128(3.29)</sup> (TMIII), Gln<sup>131(3.32)</sup> (TMIII), Trp<sup>206</sup> (ECL2), Phe<sup>283(6.51)</sup> (TMVI), and Gln<sup>287(6.55)</sup> (TMVI). Asp<sup>204</sup> forms a salt bridge with Lys<sup>128(3.29)</sup> and hydrogen bonds with Gln<sup>131(3.32)</sup>, both in TMIII (Fig. 4C). These interactions with Lys<sup>128(3.29)</sup> and Gln<sup>131(3.32)</sup> are preserved in the conservative substitution [D204E]V<sub>1a</sub>R (not shown), consistent with the wild-type pharmacological profile (Table 1). Removal of the negative charge at this locus ([D204A]V<sub>1a</sub>R) resulted in a decrease in both AVP affinity and signaling potency (Fig. 3D and Table 1). MD simulation of [D204A]V<sub>1a</sub>R revealed that removal of the negative charge breaks the wild-type contacts between ECL2 and TMIII (Fig. 4D). This leads to a partial unfolding of the β-hairpin within ECL2 (Fig. 4E). In addition, the side chain of Lys<sup>128</sup> rotates away from its wild-type position and orientates toward TMVI (Fig. 4D). A similar per-

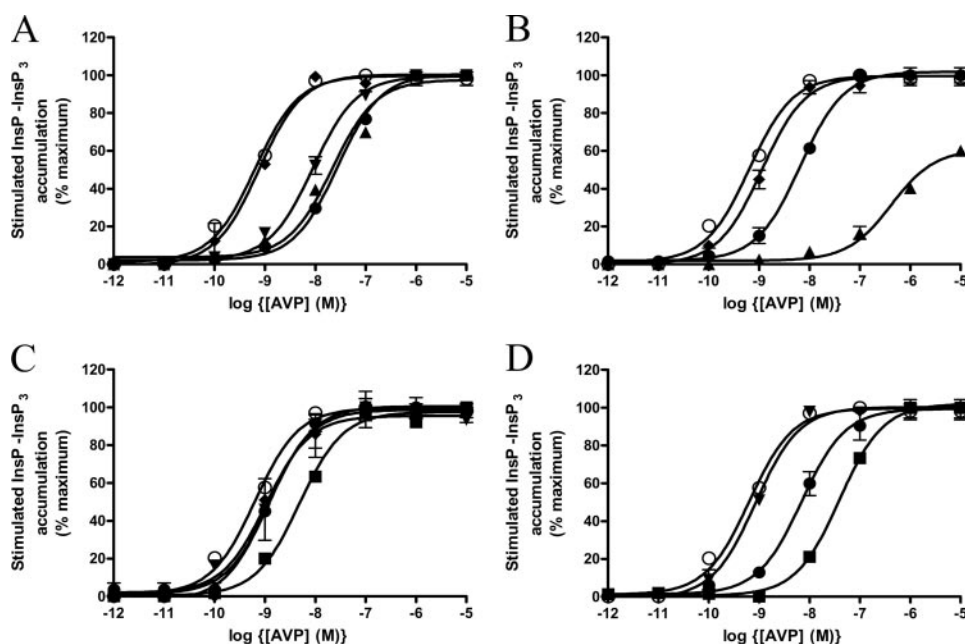


FIGURE 3. **Intracellular signaling by ECL mutant receptors.** AVP-induced accumulation of mono-, bis-, and trisphosphates in HEK 293T cells transiently transfected as follows. *A*, wild-type (Arg<sup>116</sup>) V<sub>1a</sub>R (○); [R116A]V<sub>1a</sub>R (●); [R116E]V<sub>1a</sub>R (▼); [R116D]V<sub>1a</sub>R (▲); and [R116K]V<sub>1a</sub>R (◆). *B*, wild-type (Arg<sup>125</sup>) V<sub>1a</sub>R (○); [R125A]V<sub>1a</sub>R (●); [R125D]V<sub>1a</sub>R (▲); and [R125K]V<sub>1a</sub>R (◆). *C*, wild-type (Asp<sup>112</sup>) V<sub>1a</sub>R (○); [D112A]V<sub>1a</sub>R (●); [D112E]V<sub>1a</sub>R (▼); [D112K]V<sub>1a</sub>R (◆); and [D112R]V<sub>1a</sub>R (■). *D*, wild-type (Asp<sup>204</sup>) V<sub>1a</sub>R (○); [D204A]V<sub>1a</sub>R (●); [D204E]V<sub>1a</sub>R (▼); and [D204R]V<sub>1a</sub>R (■). Data are the mean ± S.E. of three separate experiments each performed in triplicate. Values are stimulation induced by AVP at the stated concentrations expressed as percent maximum.

turbation was observed with the construct [D204R]V<sub>1a</sub>R, again leading to re-organization of ECL2. However, the introduction of an Arg at residue 204 also created an alternative hydrogen bonding network involving new interactions between Arg<sup>204</sup> in ECL2 and residues in TMII (Gln<sup>104(2.57)</sup> and Gln<sup>108(2.61)</sup>) and TMVII (Ala<sup>272(7.42)</sup> and Ser<sup>273(7.43)</sup>) (Fig. 4F).

**Role of Charged Residues in ECL3 of the V<sub>1a</sub>R**—ECL3 (including the extracellular borders of TMVI and TMVII) of the V<sub>1a</sub>R contains three conserved charged residues Asp<sup>323</sup>, Asp<sup>330</sup>, and Glu<sup>332</sup> (Fig. 1B). Analysis of sequence alignments of ECL3 of the vertebrate VPR/OTR family revealed the following: (i) an Asp is completely conserved at the locus corresponding to Asp<sup>323</sup>; (ii) a negative charge (usually an Asp) is conserved at residue 330 in V<sub>1a</sub>Rs, V<sub>1b</sub>Rs, and VTRs but is replaced by Pro in OTRs and V<sub>2</sub>Rs; and (iii) a Glu is conserved at the locus corresponding to Glu<sup>332</sup> with the exception of V<sub>1b</sub>Rs that possess a Thr (Fig. 1A). To determine the functional importance of these residues, each residue was mutated individually to Ala. Pharmacological characterization established that [D323A]V<sub>1a</sub>R, [D330A]V<sub>1a</sub>R, and [E332A]V<sub>1a</sub>R were almost identical to wild-type V<sub>1a</sub>R with respect to binding all four classes of ligand (Table 1) and intracellular signaling (Table 1), indicating that the conserved charged residues in ECL3 had little or no role in these functions. However, it was noteworthy that [D323A]V<sub>1a</sub>R exhibited reduced cell-surface expression (~50%) compared with wild-type V<sub>1a</sub>R (Table 1).

## DISCUSSION

The aim of this study was to use the V<sub>1a</sub>R to systematically investigate the function of extracellular charged residues that are highly conserved throughout a subfamily of peptide GPCRs.

Within the ECL domains of the V<sub>1a</sub>R, the charged residues were subdivided into the following two groups: (i) those that are conserved in all members of the subfamily, and (ii) those that are conserved within a specific subtype. Thirteen conserved charged residues were identified in the ECL domains and associated TM boundaries, with five in ECL1, five in ECL2, and three in ECL3. Ala substitution within ECL1 had little effect on ligand binding. However, [R116A]V<sub>1a</sub>R and [R125A]V<sub>1a</sub>R exhibited impaired intracellular signaling (70- and 16-fold, respectively) indicating a role in receptor activation. Although [R125A]V<sub>1a</sub>R was expressed at 56% of wild type, this was unlikely to be responsible for the impaired signaling of [R125A]V<sub>1a</sub>R, as [D323A]V<sub>1a</sub>R was expressed at 52% of wild type but retained essentially wild-type signaling capability (Table 1). A positive charge is essential at residue 116, as retaining a positive charge

([R116K]V<sub>1a</sub>R) preserved wild-type signaling, and reversing the charge ([R116D]V<sub>1a</sub>R and [R116E]V<sub>1a</sub>R) not only compromised signaling but also profoundly decreased agonist affinity. This loss of AVP binding was agonist-specific and not because of aberrant assembly of the receptor as the binding of antagonists (peptide and nonpeptide) was unaffected. Consequently, Arg<sup>116</sup> is required to stabilize the active R\* conformation of the V<sub>1a</sub>R and is absolutely conserved throughout the vertebrate neurohypophysial hormone subfamily of GPCRs cloned to date (Fig. 1A).

Arg<sup>125</sup> is located close to the extracellular end of TMIII, immediately adjacent to the conserved disulfide bond, where it interacts with lipids. This Arg-lipid interaction has been referred to as “snorkeling” (35). The absolute conservation of this Arg throughout the neurohypophysial peptide hormone receptor family (Fig. 1A) implies functional importance. This is supported by a report that the naturally occurring mutation R113W in the human V<sub>2</sub>R (which corresponds to Arg<sup>125</sup> in the V<sub>1a</sub>R) causes the receptor dysfunction responsible for nephrogenic diabetes insipidus in some patients (36). Furthermore, an alignment of 717 sequences of family A GPCRs, which bind peptide ligands, revealed that a positively charged residue is conserved at this position in 85% of receptors and that Asp and Glu are excluded (see the GPCR data base). This is indicative of a generic role for this residue in signaling by peptide-GPCRs, a notion supported by mutagenesis studies on the CXCR2 and angiotensin II type 1 receptors (37, 38). It is now well established that relative movement between TMIII, TMVI, and TMVII is central to the R → R\* transition of GPCRs (39). The location of Arg<sup>125</sup> at the extracellular extremity of TMIII may allow it to act as a structural support for TMIII during receptor



## Conserved Exofacial Charged Residues

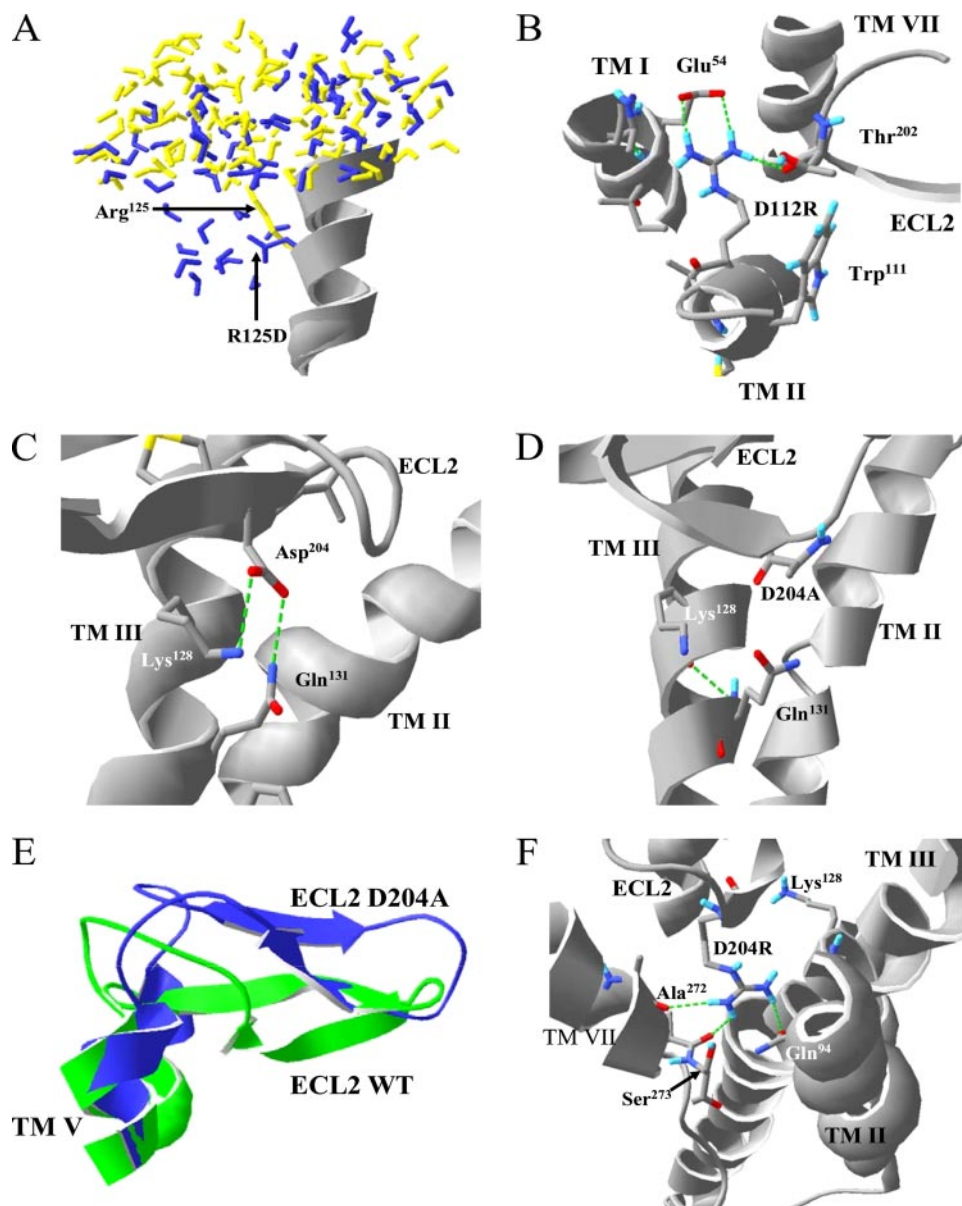


**FIGURE 4. Molecular modeling of wild-type and mutant receptors.** *A*, the overlapped positions of solvent molecules are presented for wild-type  $V_{1a}R$  (yellow) and [R125D] $V_{1a}R$  (blue) simulations. It can be seen that the mutation [R125D] $V_{1a}R$  increased the solvent-accessible surface as a result of re-ordering of the phospholipids surrounding the extracellular end of TMIII. *B*, the mutant [D112R] $V_{1a}R$  enabled inappropriate hydrogen bonds (dotted green lines) to be formed between this residue and Glu<sup>54</sup> in TMI. *C*, in the wild-type  $V_{1a}R$ , Asp<sup>204</sup> in ECL2 hydrogen bonds (dotted green lines) with Lys<sup>128</sup> and Gln<sup>131</sup> in TMIII. These contacts are broken in the mutant [D204A] $V_{1a}R$  (*D*) which results in partial unfolding of the  $\beta$ -hairpin structure of ECL2. *E*, the partially unfolded ECL2  $\beta$ -hairpin structure of [D204A] $V_{1a}R$  (blue) is revealed when superimposed onto that of wild-type  $V_{1a}R$  (yellow). *F*, the mutant [D204R] $V_{1a}R$  inappropriately hydrogen bonds (dotted green) with residues in TMVII and TMIII. See text for details.

activation. Reversing the charge at this locus in [R125D] $V_{1a}R$  was very detrimental because of charge-charge repulsion between the side-chain carboxyl and the membrane lipid phosphate head groups. This repulsion resulted in re-ordering of the surrounding phospholipids, increased solvent accessibility at the extracellular end of TMIII/TMIV, and altered local conformation that could have ramifications along the length of TMIII. These conformational changes observed *in silico* would explain why Asp/Glu are excluded from this locus in peptide-binding GPCRs. In marked contrast, GPCRs for biogenic amines actually favor a negatively charged residue at the position corre-

sponding to Arg<sup>125</sup>. Analysis of an alignment of 371 sequences of amine-GPCRs from different species revealed that ~70% have Glu/Asp at this locus (GPCR data base) with the exclusion of Arg/Lys. Exceptions to this trend are the H<sub>3</sub> histamine receptor and trace amine receptors that do possess a positive charge. It is possible that the charge difference at this single locus between peptide-GPCRs and amine-GPCRs may reflect differences in the binding mode between these ligands. Biogenic amines access a binding site enclosed within the TM bundle, whereas peptides bind to extracellular domains plus TM helices. If Glu/Asp at the top of TMIII in amine-GPCRs (corresponding to Arg<sup>125</sup> in  $V_{1a}R$ ) increases solvent penetration into the TM bundle (analogous to the mutant [R125D] $V_{1a}R$ ), it may facilitate ligand access to the binding site. Support for such a mechanism is perhaps provided by [<sup>3</sup>H]propylbenzylcholine mustard ([<sup>3</sup>H]PrBCM) labeling of the M<sub>1</sub> mAChR. In addition to alkylating Asp<sup>105</sup> in TMIII (the “classical” amine counter-ion), [<sup>3</sup>H]PrBCM also labeled Asp<sup>99</sup> (corresponding to Arg<sup>125</sup> in the  $V_{1a}R$ ) (40). Furthermore, mutation of this Asp<sup>99</sup> to Asn moderately decreased the affinity of a range of ligands and strongly decreased both alkylation by [<sup>3</sup>H]PrBCM and agonist-induced second messenger generation (41).

Asp<sup>112</sup> in the  $V_{1a}R$  is conserved throughout the neurohypophysial hormone receptor family with the exception of the human  $V_2R$  and the VTR that possess Lys and Glu, respectively. It has been reported that this locus is important for binding some  $V_2R$ -selective agonists (42).

The substitutions [D112A] $V_{1a}R$ , [D112E] $V_{1a}R$ , and [D112K] $V_{1a}R$  had little effect on receptor function; introducing Arg<sup>112</sup>, however, impaired agonist binding and signaling but had little effect on any antagonist binding. Although Arg and Lys are superficially similar, [D112K] $V_{1a}R$  and [D112R] $V_{1a}R$  exhibited very different affinity for AVP. Molecular modeling revealed that Arg<sup>112</sup> formed a stable ionic interaction with Glu<sup>54(1.35)</sup> at the top of TMI, which was absent with the shorter side chain of Lys<sup>112</sup> (and also absent in wild type and [D112E] $V_{1a}R$ ). Glu<sup>54(1.35)</sup> has recently been identified as a key residue for high affinity agonist binding and signaling (15); consequently, an inappropriate interaction with Arg<sup>112</sup>

may prevent Glu<sup>54(1.35)</sup> from adopting an optimal conformation for AVP binding and signaling.

ECL2 is usually the longest ECL in GPCRs and in bRho forms a  $\beta$ -hairpin that projects into the binding crevice allowing the  $\beta$ 4-strand to contact retinal (1, 2). There is also evidence that this ECL2 fold is not restricted to bRho and occurs in other GPCRs (43). Of the five conserved charged residues substituted by Ala in ECL2 of the V<sub>1a</sub>R, only [D204A]V<sub>1a</sub>R had a marked effect on receptor function, with a profound decrease in AVP affinity, decreased LA affinity, and impaired signaling potency. Molecular modeling revealed that Asp<sup>204</sup> provides interactions between ECL2 and TMIII by hydrogen bonding with Gln<sup>131(3.32)</sup> and forming a salt bridge with Lys<sup>128(3.29)</sup>. Substitution by Ala in [D204A]V<sub>1a</sub>R disrupted this contact network resulting in partial unfolding of ECL2 and re-arrangement of the Lys<sup>128(3.29)</sup> side chain. Substitution of Lys<sup>128(3.29)</sup> or Gln<sup>131(3.32)</sup> by Ala also disrupted AVP binding and signaling (8), consistent with the proposed role for Asp<sup>204</sup>. The reduction in affinity of both AVP and LA was similar following either removal of the negative charge ([D204A]V<sub>1a</sub>R) or charge reversal ([D204R]V<sub>1a</sub>R) (Table 1). Although [D204R]V<sub>1a</sub>R and [D204A]V<sub>1a</sub>R had the same affinity for AVP, the decrease in potency of AVP-stimulated InsP-InsP<sub>3</sub> production was greater with Arg<sup>204</sup> than with Ala<sup>204</sup> (Table 1), suggesting that Arg<sup>204</sup> stabilized the receptor ground state. Molecular modeling indicated that for both of these constructs the interactions between ECL2 and TMIII were disrupted in a similar manner leading to re-organization of ECL2. However, the introduction of the longer side chain of Arg<sup>204</sup> also created new interactions between ECL2-TMII (Gln<sup>104(2.57)</sup> and Gln<sup>108(2.61)</sup>) and ECL2-TMVII (Ala<sup>272(7.42)</sup> and Ser<sup>273(7.43)</sup>), which reduced the R  $\rightarrow$  R\* transition. Interestingly, Ser<sup>273(7.43)</sup> corresponds to the retinal attachment site in bRho, and this locus has been implicated in activation of other GPCRs (44, 45). In addition, Ala substitution of both of the TMII contacts, Gln<sup>104(2.57)</sup> and Gln<sup>108(2.61)</sup>, has been reported previously to perturb both ligand binding and intracellular signaling (8). Consequently, the inappropriate new contacts established by Arg<sup>204</sup> are with residues required for receptor activation and explain the perturbed pharmacological profile observed with [D204R]V<sub>1a</sub>R. In contrast, the conservative substitution [D204E]V<sub>1a</sub>R, which occurs naturally in a chick VTR (33), maintains the normal ECL2-TMIII contacts and exhibits wild-type characteristics. Our investigations establish the importance of an acidic residue at position 204 and provide an explanation for the absolute conservation of Asp(Glu) at this locus throughout a subfamily of GPCRs. In addition, our study also provides a feasible mechanism for the naturally occurring "loss-of-function" mutation D191G in the human V<sub>2</sub>R (corresponding to Asp<sup>204</sup> in the V<sub>1a</sub>R) that has been identified as a cause of nephrogenic diabetes insipidus in some families (46). Asp<sup>204</sup> is juxtaposed to the disulfide bridge (Cys<sup>205</sup>), conserved in the majority of GPCRs, and is therefore under positional restraint. Interestingly, the residue corresponding to Asp<sup>204</sup> has been reported to be functionally important in other GPCRs. For example, Met<sup>195</sup> of the cholecystokinin-A receptor is required for interaction with cholecystokinin (47), and the mutation I185A affected CXCR4 co-re-

ceptor activity for some human immunodeficiency virus strains (48).

The functional importance of Asp<sup>204</sup> for agonist binding and signaling by V<sub>1a</sub>R is a property shared by Arg<sup>125</sup> (this study) and also Arg<sup>46</sup> in the N terminus (14). It was therefore possible that a charge-charge interaction between Arg<sup>125</sup>-Asp<sup>204</sup> or Arg<sup>46</sup>-Asp<sup>204</sup> was required for high affinity agonist binding. Interaction between these two charge pairs was theoretically possible as Arg<sup>125</sup>-Asp<sup>204</sup> is located at opposite ends of the same disulfide bond, and in bRho the N terminus has been shown to make multiple contacts with ECL2 (1, 2). However, the double-reciprocal mutants [R125D/D204R]V<sub>1a</sub>R and [R46D/D204R]V<sub>1a</sub>R were both severely compromised; therefore, our data do not support a direct interaction of Asp<sup>204</sup> with either Arg<sup>125</sup> or Arg<sup>46</sup>.

Although ECL3 charged residues are important for peptide ligands binding to some GPCRs (49–51), substitution of the three conserved charged residues in ECL3 of the V<sub>1a</sub>R did not affect either ligand binding or activation of the receptor. However, the mutant [D323A]V<sub>1a</sub>R did exhibit decreased cell-surface expression (~50% of wild type). It is noteworthy that Asp<sup>323</sup> is the only ECL3 charged residue absolutely conserved throughout the vertebrate neurohypophysial hormone receptors cloned to date, suggesting that it may fulfill an important role in maintaining cell-surface expression that is common to all members of this family. Our data do not support the suggestion (52) that ECL3 acidic residues might be implicated in binding AVP and vasotocin.

In conclusion, we have shown that key charged residues located throughout the extracellular face of the V<sub>1a</sub>R are required for normal receptor function, identifying Arg<sup>116</sup> (ECL1), Arg<sup>125</sup> (top of TMIII), and Asp<sup>204</sup> (ECL2) as important for high affinity agonist binding and/or receptor activation and Asp<sup>323</sup> (ECL3) as important for cell-surface expression. Consistent with their fundamental role in receptor function, these charged residues are highly conserved throughout the neurohypophysial hormone receptor subfamily of GPCRs.

*Acknowledgment*—We are grateful to Dr. Claudine Serradeil-Le Gal (Sanofi Recherche, France) for providing a sample of SR 49059.

## REFERENCES

1. Palczewski, K., Kumasaka, T., Hori, T., Behnke, C. A., Motoshima, H., Fox, B. A., Le Trong, L., Teller, D. C., Okada, T., Stenkamp, R. E., Yamamoto, M., and Miyano, M. (2000) *Science* **289**, 739–745
2. Li, J., Edwards, P. C., Burghammer, M., Villa, C., and Schertler, G. F. X. (2004) *J. Mol. Biol.* **343**, 1409–1438
3. Lu, Z. L., Saldanha, J. W., and Hulme, E. C. (2002) *Trends Pharmacol. Sci.* **23**, 140–146
4. Thibonnier, M., Coles, P., Thibonnier, A., and Shoham, M. (2001) *Annu. Rev. Pharmacol. Toxicol.* **41**, 175–202
5. Gimpl, G., and Fahrenholz, F. (2001) *Physiol. Rev.* **81**, 629–683
6. Howl, J., and Wheatley, M. (1995) *Gen. Pharmacol.* **26**, 1143–1152
7. Hibert, M., Hoflack, J., Trumpp-Kallmeyer, S., Mouillac, B., Chini, B., Mahe, E., Cotte, N., Jard, S., Manning, M., and Barberis, C. (1999) *J. Recept. Signal. Transduct. Res.* **19**, 589–596
8. Mouillac, B., Chini, B., Balestre, M.-N., Elands, J., Trump-Kallmeyer, S., Hoflack, J., Hibert, M., Jard, S., and Barberis, C. (1995) *J. Biol. Chem.* **270**, 25771–25777
9. Howl, J., and Wheatley, M. (1996) *Biochem. J.* **317**, 577–582

## Conserved Exofacial Charged Residues

10. Kojro, E., Eich, P., Gimpl, G., and Fahrenholz, F. (1993) *Biochemistry* **32**, 13537–13544
11. Chini, B., Mouillac, B., Ala, Y., Balestre, M.-N., Trump-Kallmeyer, S., Hoflack, J., Elands, J., Hibert, M., Manning, M., Jard, S., and Barberis, C. (1995) *EMBO J.* **14**, 2176–2182
12. Hawtin, S. R., Wesley, V. J., Parslow, R. A., Patel, S., and Wheatley, M. (2000) *Biochemistry* **39**, 13524–13533
13. Hawtin, S. R., Howard, H. C., and Wheatley, M. (2001) *Biochem. J.* **354**, 465–472
14. Hawtin, S. R., Wesley, V. J., Parslow, R. A., Simms, J., Miles, A., McEwan, K., and Wheatley, M. (2002) *Mol. Endocrinol.* **16**, 600–609
15. Hawtin, S. R., Wesley, V. J., Simms, J., Argent, C. C. H., Latif, K., and Wheatley, M. (2005) *Mol. Endocrinol.* **19**, 2871–2881
16. Wesley, V. J., Hawtin, S. R., Howard, H. C., and Wheatley, M. (2002) *Biochemistry* **41**, 5086–5092
17. Shi, L., and Javitch, J. A. (2002) *Annu. Rev. Pharmacol. Toxicol.* **42**, 437–467
18. Ding, X. Q., Pinon, D. I., Furse, K. E., Lybrand, T. P., and Miller, L. J. (2002) *Mol. Pharmacol.* **61**, 1041–1052
19. Zhao, M. M., Hwa, J., and Perez, D. M. (1996) *Mol. Pharmacol.* **50**, 1118–1126
20. Gnagey, A. L., Seidenberg, M., and Ellis, J. (1999) *Mol. Pharmacol.* **56**, 1245–1253
21. Ott, T. R., Troskie, B. E., Roeske, R. W., Illing, N., Flanagan, C. A., and Millar, R. P. (2002) *Mol. Endocrinol.* **10**, 1079–1088
22. Brelot, A., Heveker, N., Montes, M., and Alizon, M. (2000) *J. Biol. Chem.* **275**, 23736–23744
23. Hawtin, S. R., Tobin, A., Patel, S., and Wheatley, M. (2001) *J. Biol. Chem.* **276**, 38139–38146
24. Howl, J., Langel, Ü., Hawtin, S. R., Valkna, A., Yarwood, N. J., Saar, K., and Wheatley, M. (1997) *FASEB J.* **11**, 582–590
25. Kruszynski, M., Lammek, B., Manning, M., Seto, J., Haldar, J., and Sawyer, W. H. (1980) *J. Med. Chem.* **23**, 364–368
26. Cheng, Y., and Prusoff, W. H. (1973) *Biochem. Pharmacol.* **22**, 3099–3108
27. Conner, A. C., Hay, D. L., Simms, J., Howitt, S. G., Schindler, M., Smith, D. M., Wheatley, M., and Poyner, D. R. (2005) *Mol. Pharmacol.* **67**, 20–31
28. Thompson, J. D., Higgins, D. G., and Gibson, T. J. (1994) *Nucleic Acids Res.* **22**, 4673–4680
29. Sali, A., and Blundell, T. L. (1993) *J. Mol. Biol.* **234**, 779–815
30. Lindahl, E., Hess, B., and van der Spoel, D. (2001) *J. Mol. Med.* **7**, 306–317
31. Schmidt, A., Audigier, S., Barberis, C., Jard, S., Manning, M., Kolodziejczyk, A. S., and Sawyer, W. H. (1991) *FEBS Lett.* **282**, 77–81
32. Serradeil-Le Gal, C., Wagon, J., Garcia, C., Lacour, C., Guiraudou, P., Christophe, B., Villanova, G., Nisato, D., Maffrand, J. P., and Le Fur, G. P. (1993) *J. Clin. Investig.* **92**, 224–231
33. Tan, F.-L., Lolait, S. J., Brownstein, M. J., Saito, N., MacLeod, V., Baeyens, D. A., Mayeux, P. R., Jones, S. M., and Cornett, L. E. (2000) *Biol. Reprod.* **62**, 8–15
34. Hawtin, S. R., Wesley, V. J., Simms, J., Parslow, R. A., Simms, J., Miles, A., McEwan, K., Keen, M., and Wheatley, M. (2003) *Eur. J. Biochem.* **270**, 4681–4688
35. Strandberg, E., and Killian, J. A. (2003) *FEBS Lett.* **544**, 69–73
36. Birnbaumer, M., Gilbert, S., and Rosenthal, W. (1994) *Mol. Endocrinol.* **8**, 886–894
37. Katancik, J. A., Sharma, A., and de Nardin, E. (2000) *Cytokine* **12**, 1480–1488
38. Monnot, C., Bihoreau, C., Conchon, S., Curnow, K. M., Corvol, P., and Clauser, E. (1996) *J. Biol. Chem.* **271**, 1507–1513
39. Schwartz, T. W., Frimurer, T. M., Holst, B., Rosenkilde, M. M., and Elling, C. E. (2006) *Annu. Rev. Pharmacol. Toxicol.* **46**, 481–519
40. Kurtenbach, E., Curtis, C. A. M., Pedder, E. K., Aitken, A., Harris, A. C. M., and Hulme, E. C. (1990) *J. Biol. Chem.* **265**, 13702–13708
41. Fraser, C. M., Wang, C.-D., Robinson, D. A., Gocayne, J. D., and Venter, J. C. (1989) *J. Biol. Chem.* **36**, 840–847
42. Cotte, N., Balestre, M. N., Phalipou, S., Hibert, M., Manning, M., Barberis, C., and Mouillac, B. (1998) *J. Biol. Chem.* **273**, 29462–29468
43. Shi, L., and Javitch, J. A. (2004) *Proc. Natl. Acad. Sci. U. S. A.* **101**, 440–445
44. Marie, J., Richard, E., Pruneau, D., Paquet, J.-L., Siatka, C., Larguier, R., Ponce, C., Vassault, P., Groblewski, T., Maignet, B., and Bonnafous, J.-C. (2001) *J. Biol. Chem.* **276**, 41100–41111
45. Lu, Z.-L., Saldanha, J. W., and Hulme, E. C. (2001) *J. Biol. Chem.* **276**, 34098–34104
46. Arthus, M.-F., Lonergan, M., Crumley, M. J., Naumova, A. K., Morin, D., De Marco, L. A., Kaplan, B. S., Robertson, G. L., Sasaki, S., Morgan, K., Bichet, D. G., and Fujiwara, T. M. (2000) *J. Am. Soc. Nephrol.* **11**, 1044–1054
47. Gigoux, V., Escricout, C., Silvente-Poirot, S., Maignet, B., Gouilleux, L., Fehrentz, J. A., Gully, D., Moroder, L., Vaysse, N., and Fourmy, D. (1998) *J. Biol. Chem.* **273**, 14380–14386
48. Brelot, A., Heveker, N., Adema, K., Hosie, M. J., Willett, B., and Alizon, M. (1999) *J. Virol.* **73**, 2576–2586
49. Gigoux, V., Escricout, C., Fehrentz, J. A., Poirot, S., Maignet, B., Moroder, L., Gully, D., Martinez, J., Vaysse, N., and Fourmy, D. (1999) *J. Biol. Chem.* **274**, 20457–20464
50. Fromme, B. J., Katz, A. A., Roeske, R. W., Millar, R. P., and Flanagan, C. A. (2001) *Mol. Pharmacol.* **60**, 1280–1287
51. Feng, Y.-H., Noda, K., Saad, Y., Liu, X.-P., Husain, A., and Karnik, S. S. (1995) *J. Biol. Chem.* **270**, 12846–12850
52. Hausmann, H., Richters, A., Kreienkamp, H.-J., Meyerhof, W., Mattes, H., Lederis, K., Zwiers, H., and Richter, D. (1996) *Proc. Natl. Acad. Sci. U. S. A.* **93**, 6907–6912
53. Ballesteros, J. A., and Weinstein, H. (1995) *Methods Neurosci.* **25**, 366–428

**Charged Extracellular Residues, Conserved throughout a G-protein-coupled Receptor Family, Are Required for Ligand Binding, Receptor Activation, and Cell-surface Expression**

Stuart R. Hawtin, John Simms, Matthew Conner, Zoe Lawson, Rosemary A. Parslow, Julie Trim, Andrew Sheppard and Mark Wheatley

*J. Biol. Chem.* 2006, 281:38478-38488.

doi: 10.1074/jbc.M607639200 originally published online September 21, 2006

---

Access the most updated version of this article at doi: [10.1074/jbc.M607639200](https://doi.org/10.1074/jbc.M607639200)

Alerts:

- [When this article is cited](#)
- [When a correction for this article is posted](#)

[Click here](#) to choose from all of JBC's e-mail alerts

This article cites 48 references, 21 of which can be accessed free at <http://www.jbc.org/content/281/50/38478.full.html#ref-list-1>